International Journal of Applied Pharmaceutics

ISSN- 0975-7058 Vol 16, Issue 5, 2024

Original Article

THE DEVELOPMENT OF METHOD FOR ACTIVATING PHARMACEUTICAL SUBSTANCES WITH SUBSEQUENT *IN SITU* STUDY OF MODIFIED POWDER PROPERTIES

ELENA USPENSKAYA, EKATERINA S. KUZMINA*, HOANG T. N. QUYNH, ALEKSEY A. TIMOFEEV, TATIANA V. MAXIMOVA

[1]Department of Pharmaceutical and Toxicological Chemistry, Medical Institute, RUDN University, Miklukho-Maklaya 8, Moscow-117198, Russia. [2,3,5]Department of Pharmaceutical and Toxicological Chemistry, Medical Institute, Peoples' Friendship University of Russia Named After Patrice Lumumba (RUDN University), Russia. [4]Institute of Biochemical Technology and Nanotechnology, Peoples' Friendship University of Russia Named After Patrice Lumumba (RUDN University), Russia

*Corresponding author: Ekaterina S. Kuzmina; *Email: kkuz11@inbox.ru

Received: 17 May 2024, Revised and Accepted: 20 Jul 2024

ABSTRACT

Objective: The aim of this work is to develop a method of activation of pharmaceutical substances by means of a mechanical load on the powder of the substance with the subsequent evaluation on site of the modified preparation. A complex of analytical methods and biotesting were used to characterize the solid-state phase transformation product.

Methods: The object of study was powder of the antiepileptic substance Lacosamide (Lcs); Mechanical Activation (MA) of Active Pharmaceutical Ingredient (API) was carried out using the Stegler LM-250 rotary knife mill; Fourier-Transform Infra-Red (FT-IR) spectroscopy in the range of 4000-400 cm^{-1} was used to analyses the band shift in the spectrum; Dynamic Laser Scattering (DLS) has been used to detect groups of particles ranging in size from 0 to 1000 nm; an innovative method of Two-Dimensional Diffuse Light Scattering (2D-DLS) was used to detect differences in the speckle structure of powder samples before and after modification; Scanning Electron Microscopy (SEM) was used to evaluate particle morphology; X-Ray Fluorescence analysis (XRF) was used to determine the elemental composition of the samples; polarimetry was used to determine the optical activity and *Spirotox* biotesting has been used to evaluate the biological activity.

Results: SEM images of the sample after activation represent a glassy, structurally amorphous state in contrast to the native state. Chemometric processing of FT-IR spectra allowed us to identify the regions of the samples at different activation times on the 2D-diagram of Principal Components Analysis (PCA). According to the XRF data, the elements Fe, Cu, and Zn are predominant in the Lcs-activated sample. The 2D-DLS method revealed differences in speckle structure between samples before and after mechanical activation. The same optical activity of the solutions of the studied samples with preservation of the chiral center was revealed. The *Spirotox* method showed a 1.6-fold ($P \leq 0.05$) increase in biological activity of the activated Lcs sample based on the calculated values of activation energy ($^{bs}E_a$) of the process of cellular transitions to the immobilized state.

Conclusion: The developed method of activation of pharmaceutical substances includes a full cycle of 90 min mechanical load chemistry duration with the description of technical equipment and conditions. The results of this study can be used in the pharmaceutical industry to produce preparations with improved physical-chemical and biopharmaceutical properties.

Keywords: Mechanical activation, Antiepileptic drug, Surface defects, Knife mill, *In situ* study, Scanning electron microscopy, Amorphization, *Spirotox* biotesting

DOI: https://dx.doi.org/10.22159/ijap.2024v16i5.51481 Journal homepage: https://innovareacademics.in/journals/index.php/ijap

INTRODUCTION

Oral delivery of drugs with low water solubility or poor metabolic stability is the main problem in the modern pharmacy [1]. The reason for the unsatisfactory bioavailability of new synthesized drugs at oral ingestion can be explained by Lipinski's rule of five, also known as Pfizer's rule of five or just Rule Five (RO5) [2-4]. Regulation RO5 defines the pharmacokinetic properties of medicinal substances such as absorption, distribution, metabolism and excretion: not more than 5 hydrogen bond donors; not more than 10 hydrogen bond acceptors; molecular mass less than 500 Da; separation coefficient is not more than 5. According to the Lipinski RO5, an orally active drug cannot have more than one condition disorder determining its effectiveness [5]. It is known that more than 40% of synthesized medicinal substances have low solubility and permeability, which means that they belong to Class IV of the Biopharmaceutical Classification System (BCS). Many promising drug candidates require physical-chemical modification-activation or special formulation technology. That is, solubility and permeability can be modulated. For example, the solubility of Active Pharmaceutical Ingredients (APIs) can be improved by metastable states, salt forms or co-crystals [6]. One of the promising approaches to changing the properties of medicinal substances is activation by grinding using special equipment-cutting, knife, impact, ball mills [7, 8]. For example, in work [9] it is reported on the solid-phase synthesis of dantrolene (agent for the treatment of malignant hyperthermia) by mechanochemistry in a single-step condensation between 5-(4-nitrophenyl) furfural and 1-aminohydantoine hydrochloride. The advantage of the method is that it can demonstrate a significantly improved environmental impact and lower costs than conventional solvent-based procedures.

Mechanochemistry opens up new possibilities in modification, creation and sieving of materials with the specified properties, in expansion of industrial production, as well as in expansion of opportunities for work in ecologically safe and practically non-responsive conditions. One of the principles of "green" (sustainable) chemistry formulated by American scientists P. Anastas and J. Warner states: «It is better to prevent the generation of waste than to recycle or destroy it» [10]. Drug activation techniques based on the concept of solvent-free solid-phase reactions and by-product formation are becoming increasingly popular as they meet the accepted European Chemicals Agency (ECHA) regulatory requirements of the American Chemical Society and the Organization for Economic Cooperation and Development [11]. The machined substance undergoes grinding and activation phases. Grinding is usually accompanied by an increase in the surface area of the powder and amortization. Mechanical activation is accompanied by energy accumulation in the form of defects in the solid and transition to plastic deformation, which helps to reduce the energy of activation of further chemical transformations involving activated solid (fig. 1) [12].

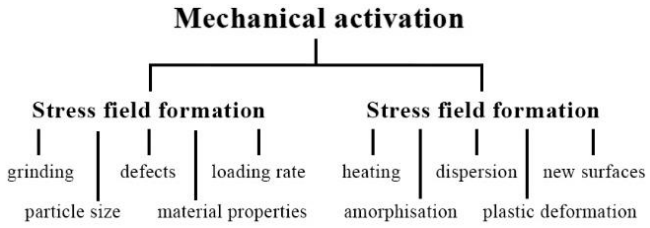

Fig. 1: Structural effects of mechanical stress on solid

Since mechanochemical reactions take place in closed plants without the possibility of open transformation management, it is advisable to study the mechanism of solid phase reactions *in situ* [13].

The aim of this work is to develop a method of activation of pharmaceutical substances with the use of an antiepileptic preparation of lacosamide (Vimpat®), which will be followed by *in situ* research of modified powder properties by physicochemical, chemometric and biopharmaceutical analysis.

MATERIALS AND METHODS

Chemicals and reagents

In this work, lacosamid produced by the Jiangsu Aimi Tech Co., Ltd. (Jiangsu China) (the content of API ≥97.5%) is presented as a white or almost white or light-yellow powder. Solubility: sparingly soluble in water, freely soluble in methanol, practically insoluble in heptane. The predicted and experimental properties of lacosamid are log Po/w (0.73), pKa (12.5) as a-NH-C=O-amid derivate, $T_{melting}$ (140-146 C), $T_{boiling}$(537 °C) (fig. 2).

Sample preparation

The solvents–deionized high resistance water (18.2 MΩ•cm at 25 °C, Milli-Q system) was used to prepare homogeneous solutions for dispersion analysis and electrokinetic stability by the Dynamic Laser Scattering (DLS) method.

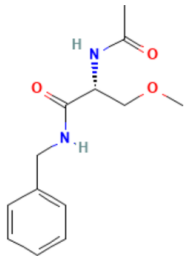

(+)-(2R)-2-acetylamino-N-benzyl-3-methoxypropanamide

Fig. 2: Lacosamide structure [14]

Methods of research

The mechanical activation cycle of the lacosamide substance powder was initiated using the rotary-type of knife laboratory mill Stegler LM-250 (Shenzhen Bestman tool CO., LTD, China). The design of the study is shown (fig. 3, table 1).

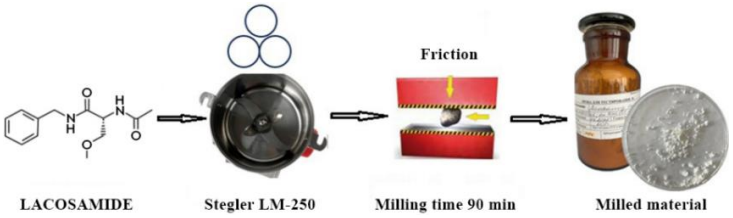

Fig. 3: Lacosamide powder mechanical activation research design scheme

Table 1: Research methods and preset activation parameters for lacosamid

Grinding capacity, g	Powder weight, g	Power, kW, rotational speed, r·min^{-1}	Common cycle of MA, (t, min)	Sample unloading step (t, min)	Methods of *in situ* analyses*
250	60	13; 28000	90	10	SEM, 2D-DLS, FT-IR, DLS,polarimetry, *Spirotox*

*The specimens of the substances have been assigned a number corresponding to their discharge time from the mechanical activator shredder with increments of time: t=10 min: lacosamid_native; Lcs_10; Lcs_20; Lcs_30; Lcs_40; Lcs_50; Lcs_60; Lcs_70; Lcs_80; Lcs_90.

Scanning electron microscopy (SEM)

The size, shape and texture of the powdered specimens of the studied substance were estimated by the method of scanning electron microscopy (LYRA3, Tescan, Brno-Kohoutovice, Czech Republic) with pre-vacuuming the samples and removing excess charge from the surface by applying an amorphous carbon layer.

2D-diffuse light scattering method (2D-DLS)

An innovative approach based on 2D-DLS reverse light scattering registration was applied to detect differences in the speckle structures of the native substance samples surface and the substance samples at the end of the mechanical activation (MA) cycle. The obtained patterns of light scattering from a surface experiencing micro-vibrations of different frequencies, depending on the external conditions of exposure, were processed using ten topological descriptors similar to the QSAR descriptors of Wiener (W) and Balaban (J) modified by Trinajstic (l), as well as, triadic: sd_1, sd_2, sd_3; r_1, r_2, r_3 (ri=di/sdi) and$R = \prod_i Ri / \sum_i Ri$ (table 2).

Dynamic light scattering (DLS)

The distribution of Lcs particles ranging in size from 0.1 to 1000 nm, their electrokinetic potential and dispersibility control in aqueous solutions before and after high-intensity mechanical loading were determined using a ZetasizerNano ZS dynamic light scattering (DLS) spectrometer (MALVERN Instruments, Malvern, UK).

Table 2: Characteristics and properties of topological descriptors

Descriptor	Mathematical representation	Definition
d_1	$\boldsymbol{d_1 = \frac{i_{\Delta Si>Sb}}{i_t} \cdot 100\%}$ It is the total number of elements. ΔSi is the value of differences in the signal level of the elements of two interference patterns. Sb is the threshold level of the signal	The number of different elements, regardless of the degree of difference
d_2	$\boldsymbol{d_2 = \frac{\sum_{\Delta Si>Sb} \Delta S_i}{i_t \cdot \overline{S}} \cdot 100\%}$ $\sum_{\Delta Si>Sb} \Delta S_i$ is the average value of the signal level of all the elements of the original interference pattern	The degree of difference for each discrete element based on the original interference pattern and the total intensity of the level of its signal
d_3	$\boldsymbol{d_3 = \frac{\sum_{\Delta Si>Sb} \Delta S_i}{i_t \cdot \Delta S_{max}} \cdot 100\%}$ $\Delta S_{max}$is the sum of possible maximum differences in terms of the signal level of all the relevant elements of the interference patterns of absolute black and absolute white	The maximum value of possible differences between the interference patterns of absolute black and absolute white

Each of the represented descriptors is a topological convolution of the light scattering matrix obtained by subtracting the background of the element behind the element and is able to reflect surface irregularities and the variability of reflected light on the dynamics.

Fourier-transform infra-red spectroscopy (FT-IR)

The analysis in the mid-infrared region was carried out using a Cary 630 Fourier transform IR spectrometer (Agilent Technologies, USA) with an ATR (attenuated total reflection) attachment.

Principal component analysis (PCA)

Chemometric PCA has been applied to efficiently detect differences in the FT-IR spectra of the studied in situ lacosamide powder samples [15] (table 3).

Table 3: Fragment of the experimental primary principal component analysis matrix (J – Variable values of wave numbers; I – Examined samples)

J							
Wavenumber, cm^{-1}	**499.613**	**500.587**	**501.444**	**502.358**	**503.343**	**504.253**	**505.122**
I							
Sample*	68.678	65.877	70.645	79.987	80.765	76.767	78.296
1	70.454	73.044	76.265	79.145	81.576	83.265	83.738
2	81.167	82.467	84.032	86.367	87.799	87.943	88.758
3	62.423	66.222	69.956	72.533	74.065	75.445	77.353
4	84.612	86.100	87.878	88.844	89.078	89.599	90.457
5	72.997	75.487	77.699	80.057	81.977	82.9789	83.033
6	68.445	71.065	73.733	76.488	78.544	80.665	82.148
7	74.721	76.932	78.545	80.522	82.567	83.667	84.225
8	76.712	78.834	80.656	82.611	84.211	85.635	85.775
9	67.356	71.056	73.9176	76.434	78.444	79.628	80.266

*Number «I» correspond to the lacosamide sample *in situ* study

As follows from the tabulated data, PCA consisted in reducing the multivariate data set-into a smaller set of variables in new coordinates. Thus, the spectral data array obtained by the FT-IR method for substance samples with different mechanical loading times, i. e. the numerical characteristics of the Transmittance, % =f (Wavenumber, cm^{-1}), were converted to primary matrix X.

Matrix X = J × Iincludes more than 3000 values of wave numbers (cm^{-1}) for 10 samples of Lcs powder with different mechanical loading times. Then, using the capabilities of the OriginPro 2021 the initial matrix X was transformed into a set of values with corresponding coordinates-PC1-PC2. The measure that determines the level of similarity between the objects is the Mahalanobis distance [17]:

$$D^2 = (x - \bar{x})^T S^{-1} (x - \bar{x})', \ldots\ldots (1)$$

Where D^2– is the Mahalanobis distance; x– vector of data; $\bar{x}$ – is the vector of mean values of the independent variables; T – is the direction vector (indicates vector should be transposed); S^{-1}–is the variance-covariance matrix of the sample; «′» – represents transposition, that is, rows and columns are swapped.

The differences between the samples were considered reliable with 95% probability if the Mahalanobis distance was at least three times the standard deviation (σ ≥3). For the processing of the results and the two-dimensional visualization of the results, the Mahalanobis distance was interpreted as the distance from the data set center (ellipse) to any point lying on the plane. Points outside the ellipse were considered distinct and incompatible with the mechanism for generating the analysis results [16].

X-ray fluorescence (XRF)

An energy-dispersive XRF spectrometer (EDX-7000P, Shimadzu Europa GmbH) based on a silicon drift detector with thermoelectric cooling and equipped with the PCEDX-Navi software package was used to study the elemental composition of lacosamide powder samples before and after the mechanical activation cycle. The range of elements measured by the X-ray fluorescence method is from 11Na to 92U; the X-ray generator is a tube with Rh anode, current 1-1000 μA; the irradiation area controlled by the collimator is 10 mm. The sample powder was placed in a cuvette covered with Mylar (lavsan) film in air atmosphere, placed in the center of the instrument window and measured. Sample "SRM 2976" manufactured at MEL IAEA (Marine Environment Laboratories of International Atomic Energy Agency) and certified by the National Institute of Standards and Technology (NIST, USA) was used as a standard reference material [17].

The formula was used to calculate the concentration of the chemical element:

$$C_X = C_{st} \cdot \frac{I_X}{I_{st}} (2),$$

Where C_X and C_{st}, I_X and I_{st}–are the element concentration (μg/g) and fluorescence intensity (cps/mA) in the test (X) and standard (st) samples, respectively.

Polarimetry

The optical activity of the aqueous solutions of lacosamide before and after activation was determined using the Atago polarimeter POL-1/2 (Japan) at wavelength λ = 589.3 nm at optical path length 100 mm and thermostatic temperature of 20 °C. For this purpose, an accurate attachment of the substance (about 0.100 g) was dissolved in 10 ml of water (background-double-distilled water):

$$[\alpha]_D^{20} = \frac{\alpha * 100}{C * l} (3),$$

Where $[\alpha]_D^{20}$-specific rotation (•ml•g^{-1}•dm^{-1}); α–the angle of rotation, °C–concentration of the tested substance solution, %; l–layer thickness (cuvette length), dm. All measurements were performed under conditions of repeatability of the methodology at n≥5, P<0.05 and measured value of standard deviation SD.

***Spirotox* method**

The study of the biological activity of Lcs as a result of mechanical activation was carried out using the *Spirostomum ambigua* test culture, characterized by statistically reliable sensitivity to toxicants. The kinetic scheme caused by ligand death of *S. ambigua* is described in **[**8] in detail. The dependence of test culture lifetime (t_L,s) on temperature (T,K) is linearized in "Arrenius coordinates"

$$k = A \cdot e^{-E_a/RT}, (4)$$

Where k – is the reaction rate constant, A-is the pre-exponential multiplier characterizing the frequency of collisions of reacting molecules, e – is the base of the natural logarithm, E_a – is the activation energy, kJ/mol; R-is the universal gas constant (8,31 J/mol• K); T – is the temperature, K.

Statistical investigation

The data has been presented in the form of the mean±standard deviation and standard error. Analytical measurements were made in n≥3, P<0.05 by Origin Pro 2021 (Origin Lab Corporation, USA).

RESULTS AND DISCUSSION

SEM research

The main reaction of a solid body to mechanical activation is deformation [18]. Structural changes may be accompanied by changes in the morphology of crystals, lattice type, increase or decrease of interatomic distances, appearance of new defects (points, linear, etc.) and amorphization [19, 20]. According to numerous studies, the amorphization of drugs through solid phase transformations contributes to a significant increase in water solubility of substances belonging to classes BCS II and IV [21].

To study the properties of the lacosamide powder at various stages of mechanical activation, SEM images of the studies surface morphology at different magnifications were obtained: particles of the lacosamid_native substance at t_{MA}=0 min are represented by needle-shaped druses with coarse surface and jagged edges their sizes vary from 30 μm to 50 μm (fig. 4).

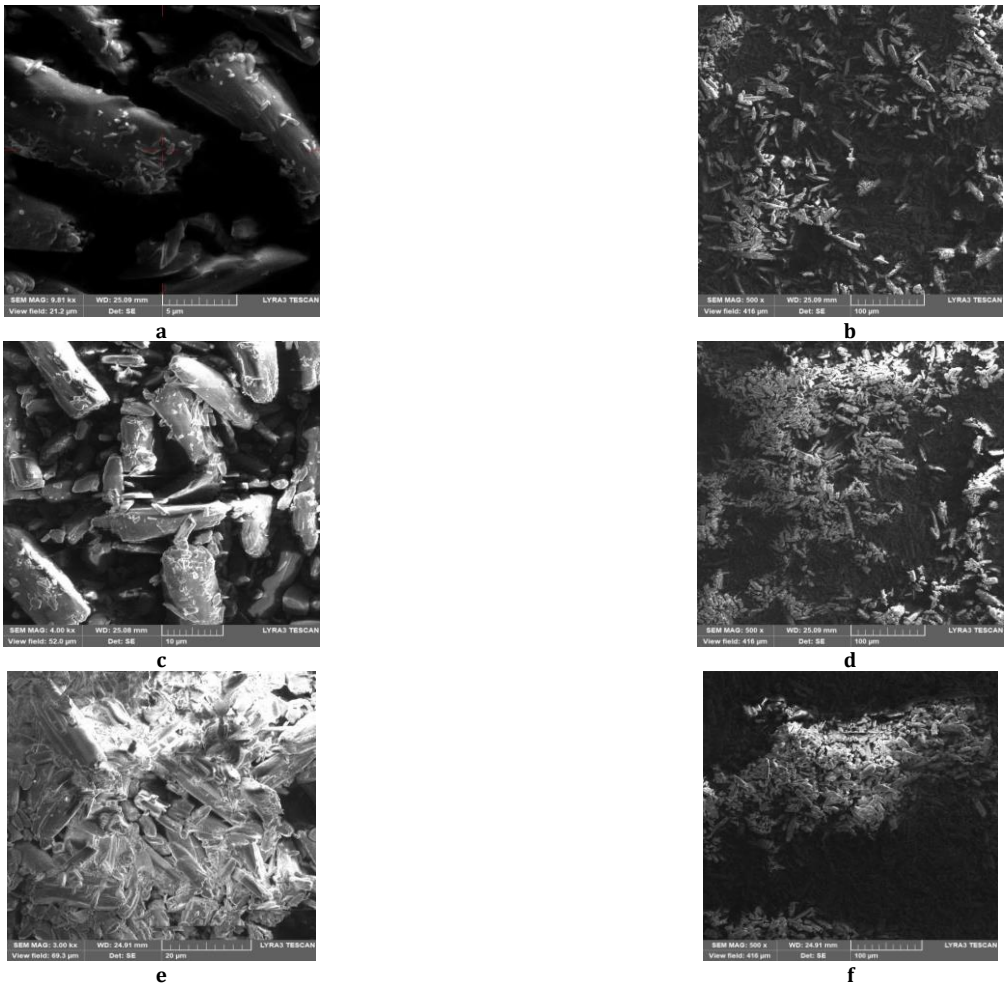

Fig. 4: Micrographs of scanning electron microscopy for lacosamid samples obtained at different times of high-intensity mechanical loading: (a,b) t=0 min; (c,d) t=60 min; (e,f) t=90 min. Magnification: 500x

Mechanical activation lasting for 60 min leads to disturbances in the surface morphology of the sample: the Lcs_60 sample is represented by much smaller particles (d ~10 μm) with a brittle surface and sharp edges with numerous trace impurities. Magnification of 500x allows us to detect numerous aggregates.

At the final stage of mechanical activation, which is 90 min, the surface of the sample acquires a glasses, structurally amorphous, isotropic state with a smooth, continuous surface with minimal morphological contrast. At 500x magnification, the presence of molten, cemented agglomerated particles is observed, which may suggest indirectly that a phase transformation of the solid has occurred [22].

It is shown [23] that such activated substances are characterized by abnormally high chemical activity, sorption capacity and low diffusion resistance. Significant energy reserves accumulated in the disordered surface layer structure cause low-temperature chemical and mechanochemical reactions [24].

Dynamic light scattering

The dispersion analysis of quasi-elastic (dynamic) dissipation based on the characteristic time of fluctuations in the intensity of scattered light in a liquid medium makes it possible to determine the physico-chemical character of fine and ultrafine grinding. When the grinding limit is reached and densely packed aggregates are formed, their internal inter-particle surface becomes inaccessible for adsorption. Formed aggregate clusters are perceived as separate particles according to dispersion analysis. High dispersion of Lcs powder after mechanical load and low colloidal stability were confirmed by the DLS method according to parameters: size distribution, Polydispersity Index (PDI), average scattering light intensity (in kilo counts per second, kcps) and ζ-potential (mV) (fig. 5, table 4).

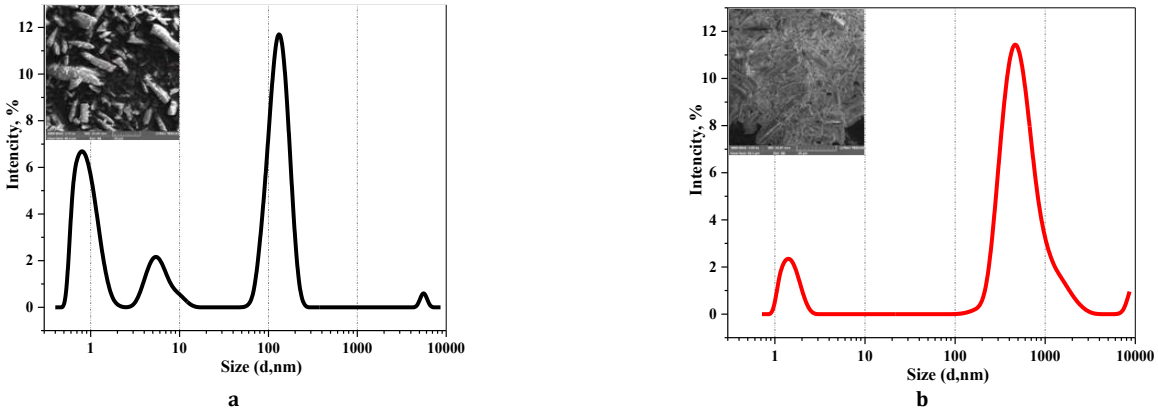

Fig. 5: Dynamics of dispersibility of the aqueous1•10^{-3}% solutions of lacosamide substances at different stages of activation: at t=0 min (a) and t=90 min (б). In insets-SEM images of the powder surface

Table 4: Dispersion properties of activated lacosamide molecular solutions

Activation time (MA), min	Size d±SD, nm	PDI±SD	Count rate, kcps	$\bar{\xi}$±SD, mV
0	d_1=0.90±0.08; d_2=7.00±0.10 d_3=103 ±2.2; d_4=6.0·10^3±1.2	0.59±0.1	326	-11.2± 0.4
90	d_1=1.4±0.10; d_2=500 ±3.1	0.33±0.1	116.4	-6.30± 0.7

n=3, (mean±SD)

Dynamic light scattering allows us to analyze changes in the conformation of disperse, anisometric, lyophilic colloidal particles in activated and initial lacosamide solutions as a time function t_{MA}: increase in mean particle diameter, decrease in polydispersion index, count rate and zeta potential values indicate swelling of nano-dispersed bicontinuous particles in aqueous solution of activated lacosamide [25].

2D-DLS

The chemometric method 2D-DLS was used to study models of light scattering from the surface of samples when their topology changed. Previously, in [26], it was found that the mechanical effect on the powder of substances changes the dynamic structure of light dissipation in coherent light and, as a consequence, changes in sintered structure. The results of the correlation method in the form of two-dimensional diagrams of multi-descriptor analysis (similar to the fingerprinting in molecular biology) illustrate the 2D-DLS (light scattering) topology for the investigated samples of lacosamide powder (fig. 6).

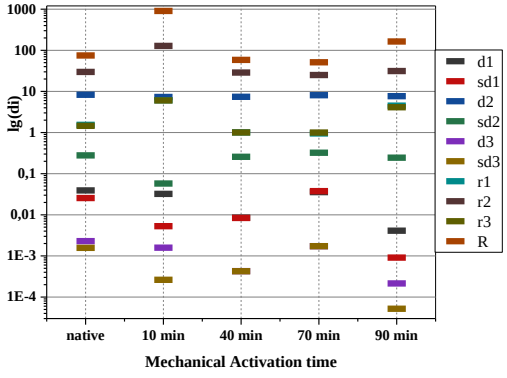

Fig. 6: "Fingerprint" diagram for lacosamide samples as a function of ten chemometric descriptors

The object of comparison is «fingerprint» sample lacosamid_native (t_{MA}=0 min), which has not gone through the mechanical loading stage. Descriptors "fingerprints" for lacosamid_native appear relatively narrow, not overlapping set. When comparing a multi-descriptor set of tested specimens with the comparison object, we used the diagnostic rule that the maximum difference between the compared descriptors should not exceed 25%; the minimum number of matching descriptors must not exceed 4.

The greatest differences are shown for the lacosamide samples activated by t_{MA}=10 min and 90 min: the set of «fingerprint» descriptors is characterized by significant variability, spanning about seven orders of magnitude along the OY axis compared to the comparable sample. The surface characteristic of the sample, which is subjected to a mechanical load for 10 min, corresponds to the fine grinding stage. The further mechanical load is accompanied by the formation of intermediate non-flow equilibrium states, deformation of the solid body and changes in the dynamic characteristics of light scattering, reaching a maximum of 90 min.

The results agree well with the results of SEM (fig. 4): solid-phase transformation of substance to vitreous state at t_{MA}=90 min corresponds to a set of descriptors for which there is maximum variability and practically no degeneration (stratification) descriptor.

XRF analysis of elements composition

One of the most important indicators for the evaluation of phase transformations at the molecular level during mechanical activation of a substance is its elemental composition. Fig. 7 shows the results of XRF elemental analysis of lacosamide samples at different stages of activation in units of fluorescence intensity and concentration.

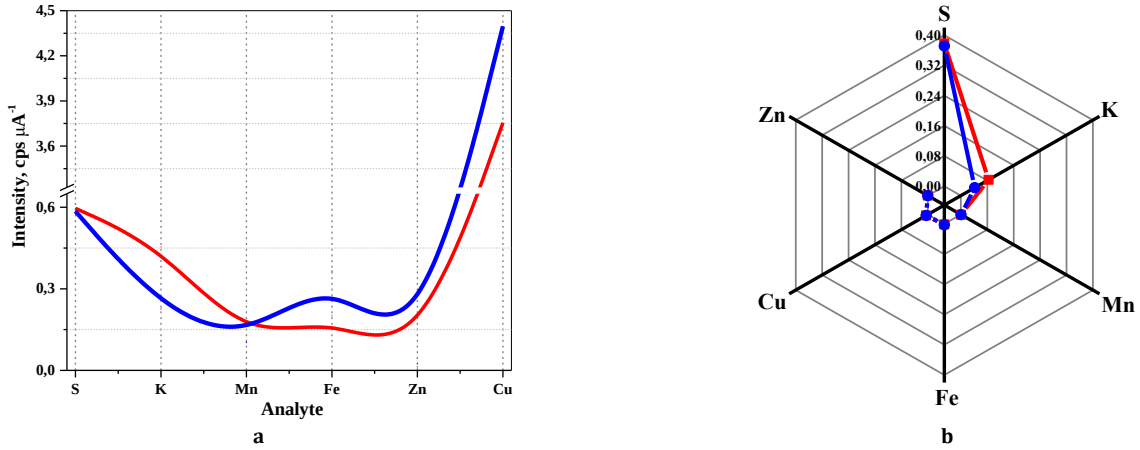

Fig. 7: X-ray fluorescence detection of elements in lacosamide-analite in units of fluorescence intensity (a); in units of concentration of the defined element (b): red curve corresponds to lacosamid_native (t_{MA}=0 min), blue curve-lacosamid_90 (t_{MA}=90) (a); in units of concentration of a certain element (b): the red curve corresponds to lacosamid_native (t_{MA}=0 min), the blue curve-lacosamid_90 min (t_{MA}=90)

It is known that when preparing the solid phase of amorphous objects their properties differ from those of the same composition in the crystalline state [27]. It draws attention to the fact that the powder of the activated substance lacosamide at the final stage of the mechanical load at tma=90 min and the transition to an amorphous (glass) phase, similar to the nanocomposite structure, are accompanied by an increase in the percentage content of elements Fe, Zn, Cu [28]. Such changes in element composition can be explained by the apparently significant qualitative and quantitative distinguishing characteristic of amorphous substances compared with the crystalline state of matter [29]. A large number of pure metals is known: Cr, Ni, Mn, Co, Ti, Pd, Y, W, Ta, Re, Nb and many alloys that become amorphous at high glazing rates [30]. Since crystalline, quasi-crystalline and amorphous substances can be regarded as systems with different energy levels, their transition from one state to another should be accompanied by structural relaxation in the amorphous phase (reduced free volume concentration) changes in crystallization energy and qualitative and quantitative element composition [31].

Fourier transform infrared spectroscopy

Deformed covalent bonds can be estimated by FT-IR. It has been shown [32] that skeletal band shift in the IR hydrocarbon spectrum in the initial state and under mechanical load can reach several waves. Fig. 8 shows the *in situ* vibrational spectra of lacosamide powder samples with different activation times. The obtained spectra reflect the peculiarities of the ongoing changes in the structure of lacosamide from the perspective of quantum-mechanical concepts.

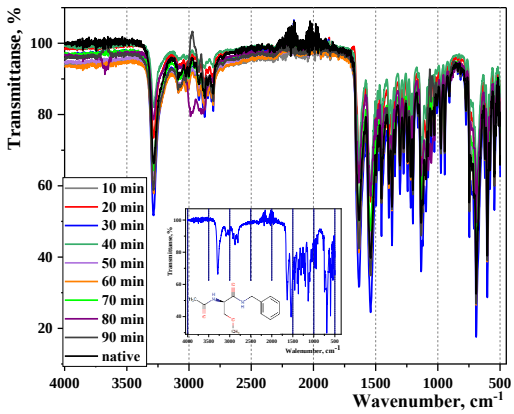

Fig. 8: Fourier transform infrared spectroscopy spectra of lacosamide samples at different stages of mechanical activation

Covalent bonds are deformed as a result of high-intensity mechanical action on a solid with hyper-or hypo-chrome effects corresponding to the excitation and vibration motion of the molecule in the harmonic oscillator model [33]. In accordance with [34], the covalent coupling deformation can be estimated by the shear of the maximum transmission/absorption bands. Chemometric treatment of FT-IR results by the main components allowed us to discover reliable differences in the vibrational spectra of lacosamide samples with different activation times. Fig. 9 shows a two-dimensional model for visualizing the results:

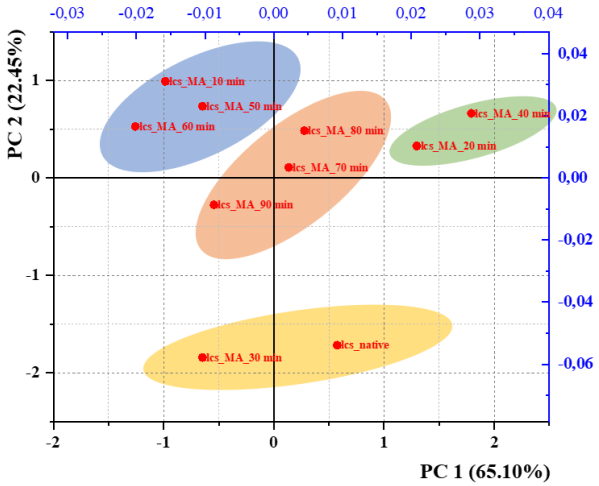

Fig. 9: 2D-diagram of principal component analysis chemometric processing of Fourier transform infrared spectroscopy method data set

2D-Diagram at "Principal Component1-Principal Component 2" ("PC1-PC2") coordinates allows to distinguish 4 clusters (groups): group I consists of lacosamid_native (initial) samples with the activation time t_{MA}=30 min; group II consists of samples with activation time t_{MA}=20 min and 40 min; group III consists of samples with activation time t_{MA}=10 min, 50 min and 60 min; (IV) group consists of samples with activation time t_{MA}=70 min 70, 80 and 90 min. The clusters occupied different regions located at Mahalanobis distance (≥3σ) from each other. The dispersion (difference) between clusters is 87.55%, 65.10% is determined by PC1 and 22.45% by PC2. Fig. 10 shows a plot of the loading matrix (P) and chemometric subtraction spectra of the original FT-IR spectra (fig. 8), which give the greatest contribution to the cluster separation procedure.

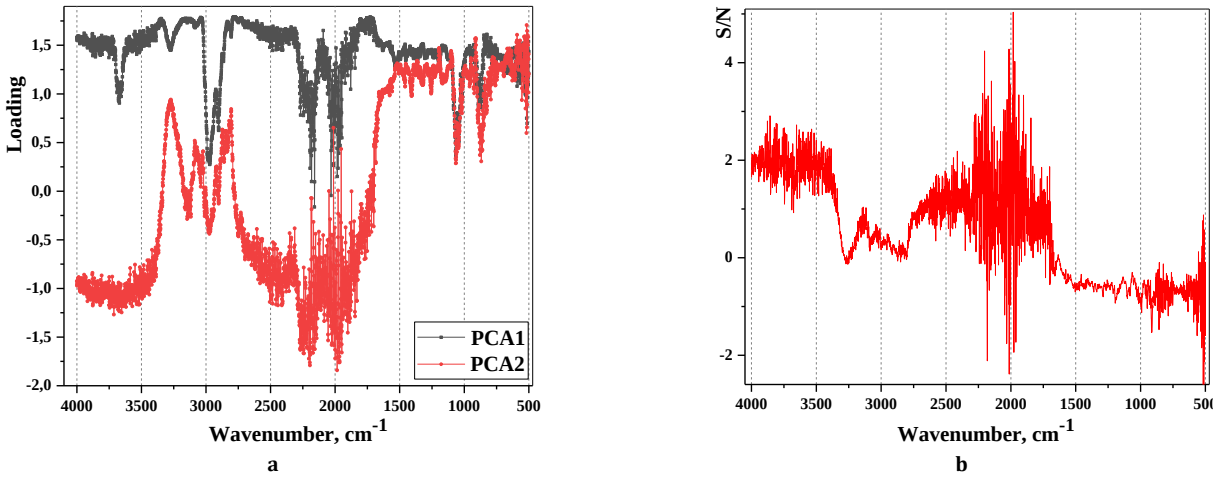

Fig. 10: Chemometric processing of fourier transform infrared spectroscopy results: principal component analysis (PCA) plot of matrix loadings (a) and "spectra subtraction" view (b) for lacosamid samples

As shown in fig. 10, the whole range of wave number values contains information on variables other than zero values and supports the procedure for splitting the cluster of samples under study. In this case, both components (PC1 and PC2) are significantly different from zero in the entire spectral range from 4000 to 500 cm^{-1}. The largest differences were recorded in the wavelength range of 3700 cm^{-1}, 2900–3000 cm^{-1}, 1750–2250 cm^{-1}, which corresponds to N-H, O-H, C=O, C=N bond vibrations (table 5).

Optical activity

It is known that the mechanism of molecular action of lacosamide is based on the interaction of its (R)-optical isomer with CRMP-2 (Collapsin Response Mediator Protein), which is most actively expressed during the development of the nervous system [35]. Whereas (S)-optical isomer does not have this ability due to the lack of stereo specificity [36].

The experiment conducted to determine the optical activity of 1% of the aqueous solutions of lacosamide obtained from samples with different activation times demonstrated the dependence of specific values of rotation in the form of harmonic oscillations, but within statistical variability: $[\alpha]_D^{20}$=+37.09±0.03(•ml•g^{-1}•dm^{-1}) for the initial substation; for the sample-loading at the end of the MA full cycle $[\alpha]_D^{20}$=+37.94±0.03(•ml•g^{-1}•dm^{-1}) (fig. 11).

Table 5: The transmittance bands in the lacosamid FT-IR spectroscopy spectra

Wavenumber, cm^{-1}	Chemical group	Compound Class	Appearance
3700–3200	O-H stretching	Alcohol	Strong
3350-3310	N-Hstretching	Secondary amine	Medium
3300-2500	O-H stretching	Carboxylic acid	Strong
1700	C=O stretching	Secondary amide	Strong
1690-1640	C=N stretching	Imine (tautomer)	Medium
1650–1580	N-H bending	Amine	Strong
1465	C-H bending	Alkane/methylene	Medium
1450-1375	C-H bending	Alkane/methyl group	Medium
1420-1330	O-H bending	Alcohol (tautomer)	Medium
1250-1020	C-N stretching	Amine	Medium
1210-1163	C-O stretching	Ester	Strong
700±20	C-H bending	Benzene derivative	Strong

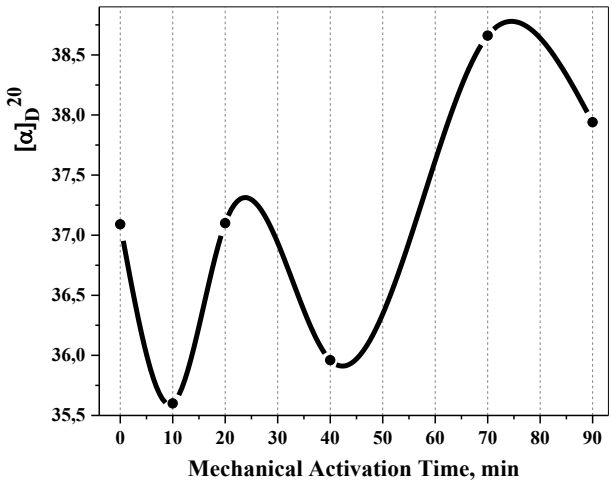

Fig. 11: Dependence of specific optical rotation in aqueous solutions of lacosamide powder samples with different activation times

The retention of optical activity at a slight change in specific rotation leads to the conclusion that the stereochemical centers in the molecule are retained.

***Spirotox*-test**

In order to demonstrate the biological effect of the mechanical activation of the lacosamide powder, a test was conducted for the cultivation of *Spirostomum ambigua* in 1% aqueous solutions. The graphical dependence in coordinates «lifetime t_L, s-T, K» is presented in the fig. 12.

Linearisation at Arrhenius coordinates $\ln(1/t_L) = f(1/T)$ allowed to calculate the values of observed activation energy ${}^{bs}E_a$ values for the dead state (DC) cell biosensor death (C_{cell}) (fig. 13, table 6).

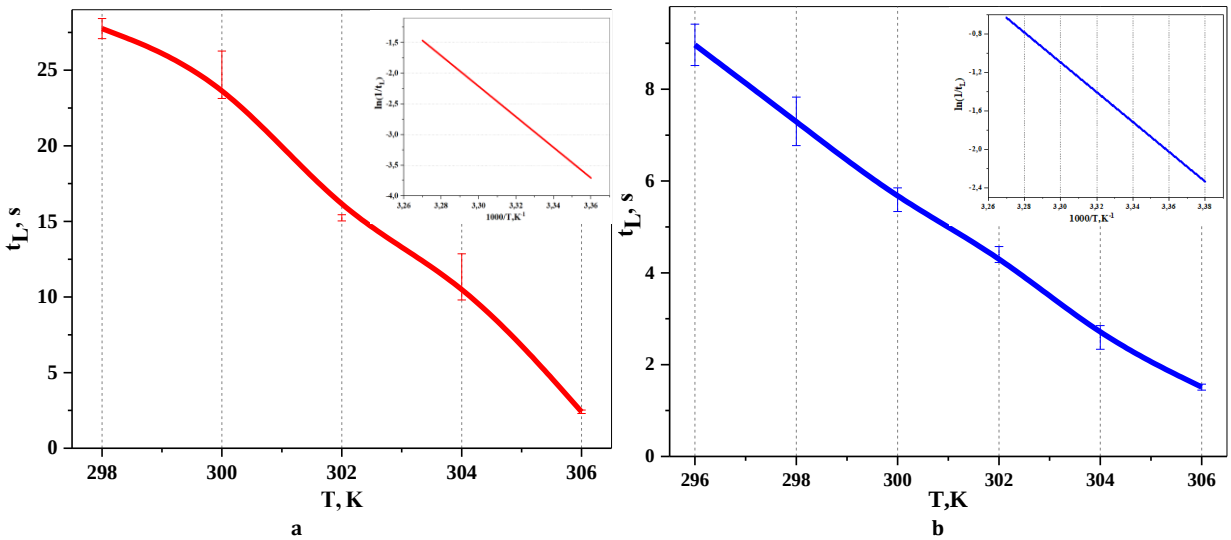

Fig. 12: Relationship of *Sp. ambigua* lifetime as a function of temperature for the samples of 0.5% water solutions: a) lacosamid_native (t_{MA}=0 min), lacosamid_90 (t_{MA}=90 min)

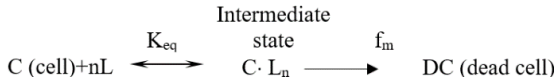

Fig. 13: The scheme of ligand-receptor interaction *Sp. ambigua* with lacosamide samples: C-cell, L-ligand, *n*-stoichiometric coefficient, $C \bullet L_n$ – intermediate state (cell after interaction with the ligand), K_{eq} is the equilibrium constant fast stage, f_m is the rate constant of the cell transition to the dead cell stage

Table 6: The observed activation energy values of ligand-induced *Sp. ambigua* death process in 0.5% water solutions of lacosamide substances-unloading samples with different MI times

Milling time, min	${}^{bs}E_a \pm SD$, kJ·mol^{-1}
0	207±1.5
90	129±0.5

n=5, (mean±SD)

The results of the Arrhenius kinetics study of cell biosensor death process in lacosamide medium by the *Spirotox* method show a 1.6-fold decrease in toxicity of aqueous solution of a full cycle activated sample of Lcs_90 drug substance with t=90 in comparison with lacosamid_native substance not subjected to mechanical loading.

CONCLUSION

The developed complex approach consisting in obtaining an activated powder of the antiepileptic drug substance lacosamide (Vimpat^{R}) and subsequent in situ study of its properties using modern physicochemical, chemometric and biopharmaceutical methods allows not only to modify drugs under conditions of solid-phase transformations but also to scale this approach for industrial production of target drugs with improved properties.

FUNDING

This publication has been supported by the RUDN University Scientific Projects Grant System, project № 033322-0-000

ACKNOWLEDGEMENT

Not applicable

FUNDING

Nil

ABBREVIATIONS

In situ-The original (primary, without movement) location of experiments, BCS-Biopharmaceutics classification system, DLS-Dynamic laser scattering, 2D-DLS-Two-dimensional dynamic backscattering, ${}^{bs}E_a$ - Observed activation energy, FT-IR-Fourier Transform Infrared spectroscopy, Lcs-Lacosamide, MA-Mechanoactivation, PCA-Principal component analysis, SEM-Scanning electron microscopy, ACS-American Chemical Society, OECD-Organization for Economic Cooperation and Development

AUTHORS CONTRIBUTIONS

Conceptualization, Data curation (Elena V. Uspenskaya); Investigation, Methodology, Writing – editing (Ekaterina S. Kuzmina); Investigation, Writing-review (Hoang Thi Ngoc Quynh); Investigation, Writing-review (Aleksey A. Timofeev); Investigation (Tatiana V. Maximova)

CONFLICT OF INTERESTS

The authors declare no other conflict of interest.

REFERENCES

1. Boyd BJ, Bergstrom CA, Vinarov Z, Kuentz M, Brouwers J, Augustijns P. Successful oral delivery of poorly water-soluble drugs both depends on the intraluminal behavior of drugs and of appropriate advanced drug delivery systems. Eur J Pharm Sci. 2019;137(1):104967. doi: 10.1016/j.ejps.2019.104967, PMID 31252052.
2. Lipinski CA, Lombardo F, Dominy BW, Feeney PJ. Experimental and computational approaches to estimate solubility and permeability in drug discovery and development settings. Adv Drug Deliv Rev. 2001;46(1-3):3-26. doi: 10.1016/s0169-409x(00)00129-0, PMID 11259830.
3. Benet LZ, Hosey CM, Ursu O, Oprea TI. BDDCS, the rule of 5 and drugability. Adv Drug Deliv Rev. 2016;1(101):89-98. doi: 10.1016/j.addr.2016.05.007, PMID 27182629.
4. Lipinski CA. Lead and drug-like compounds: the rule of five revolution. Drug Discov Today Technol. 2004;1(4):337-41. doi: 10.1016/j.ddtec.2004.11.007, PMID 24981612.
5. Jays J, Saravanan JA. Molecular modelling approach for structure-based virtual screening and identification of novel isoxazoles as potential antimicrobial agents against *S. aureus*. Int J Pharm Pharm Sci. 2024;16(4):36-41. doi: 10.22159/ijpps.2024v16i4.49731.
6. Shaikh SC, Saboo SG, Tandale PS, Memon FS, Tayade SD, Haque MA. Pharmaceutical and biomedical applications of quantum dots an overview. Int J App Pharm. 2021;13(5):44-53. doi: 10.22159/ijap.2021v13i5.41623.
7. Grejtak T, Lacey JA, Kuns MW, Hartley DS, Thompson DN, Fenske G. Improving knife milling performance for biomass preprocessing by using advanced blade materials. Wear. 2023;522(1):204714. doi: 10.1016/j.wear.2023.204714.
8. Syroeshkin AV, Uspenskaya EV, Pleteneva TV, Morozova MA, Maksimova TV, Koldina AM. Mechanochemical activation of pharmaceutical substances as a factor for modification of their physical chemical and biological properties. Int J App Pharm. 2019;11(3):118-23. doi: 10.22159/ijap.2019v11i3.32413.
9. Solares Briones M, Coyote Dotor G, Paez Franco JC, Zermeno Ortega, Dela MR. Mechanochemistry: a green approach in the preparation of pharmaceutical cocrystals. Pharmaceutics. 2021;13(6):790. doi: 10.3390/pharmaceutics13060790, PMID 34070646.
10. Warner JC, Cannon AS, Dye KM. Green chemistry. Environ Impact Assess Rev. 2004;24(7-8):775-9. doi: 10.1016/j.eiar.2004.06.006.
11. Jug M, Mura PA. Grinding as solvent free green chemistry approach for cyclodextrin inclusion complex preparation in the solid state. Pharmaceutics. 2018;10(4):189. doi: 10.3390/pharmaceutics10040189, PMID 30332804.
12. Boldyrev VV. Mechanochemistry and mechanical activation of solids. Russ Chem Rev. 2006;75(3):177-89. doi: 10.1070/RC2006v075n03ABEH001205.
13. Sovic I, Lukin S, Mestrovic E, Halasz I, Porcheddu A, Delogu F. Mechanochemical preparation of active pharmaceutical ingredients monitored by in situ raman spectroscopy. ACS Omega. 2020;5(44):28663-72. doi: 10.1021/acsomega.0c03756, PMID 33195919.
14. PubChem. PubChem Compound Summary for CID 219078, Lacosamide. Bethesda: National Library of Medicine (US). National Center for Biotechnology Information; 2004. Available from: https://pubchem.ncbi.nlm.nih.gov/compound/lacosamide. [Last accessed on 15 May 2024]
15. Munir MA, Inayatullah A, Ibrahim S, Rimba Putri IR, Emelda E, Fatmawati A. A modest uv spectrophotometric assisted by chemometric approach for verification of acetaminophen level in various manufactured tablets and syrups in Indonesian

pharmacies. Int J App Pharm. 2023;15(1):195-205. doi: 10.22159/ijap.2023v15i1.46290.

16. Li Q, Wu Z, Lin L, Zeng J, Zhang J, Yan H. High-level fusion coupled with mahalanobis distance weighted (MDW) method for multivariate calibration. Sci Rep. 2020;10(1):5478. doi: 10.1038/s41598-020-62396-y, PMID 32214179.
17. Makarova MP, Syroeshkin AV, Maksimova TV, Matveeva IS, Pleteneva TV. Features of microelements express determination in medicinal and nonoficinal plants by x-ray-fluorescence analysis. Razrabotka i Registracia Lekarstvennyh Sredstv Regist 2019;8(2):93-7. doi: 10.33380/2305-2066-2019-8-2-93-97.
18. Butyagin PY. Structural disorder and mechanochemical reactions in solids. Russ Chem Rev. 1984;53(11):1025-38. doi: 10.1070/RC1984v053n11ABEH003138.
19. Auvray T, Friscic T. Shaking things from the ground-up: a systematic overview of the mechanochemistry of hard and high melting inorganic materials. Molecules. 2023;28(2):897. doi: 10.3390/molecules28020897, PMID 36677953.
20. Speight IR, Hanusa TP. Exploration of mechanochemical activation in solid-state fluoro-grignard reactions. Molecules. 2020;25(3):570. doi: 10.3390/molecules25030570, PMID 32012963.
21. Ma D, Hettiarachchi G, Nguyen D, Zhang B, Wittenberg JB, Zavalij PY. Acyclic cucurbit[n]uril molecular containers enhance the solubility and bioactivity of poorly soluble pharmaceuticals. Nat Chem. 2012;4(6):503-10. doi: 10.1038/nchem.1326, PMID 22614387.
22. Rietveld IB. Solid-solid phase transitions between crystalline polymorphs of organic materials. Curr Pharm Des. 2023;29(6):445-61. doi: 10.2174/1381612829666221221114459, PMID 36545715.
23. Iyer J, Brunsteiner M, Modhave D, Paudel A. Role of crystal disorder and mechanoactivation in solid state stability of pharmaceuticals. J Pharm Sci. 2023;112(6):1539-65. doi: 10.1016/j.xphs.2023.02.019, PMID 36842482.
24. Lu M, Fatah N, Khodakov AY. And high optimization of solvent-free mechanochemical synthesis of Co/Al2O3 catalysts using low and high-energy processes. J Mater Sci. 2017;52(20):12031-43. doi: 10.1007/s10853-017-1299-8.
25. Engblom J, Hyde ST. On the swelling of bicontinuous lyotropic mesophases. J Phys II France. 1995;5(1):171-90. doi: 10.1051/jp2:1995121.
26. Uspenskaya E, Simutina A, Kuzmina E, Sukhanova V, Garaev T, Pleteneva T. Exploring the effects of cramped impact type mechanical action on active pharmaceutical ingredient (levofloxacin) prospects for pharmaceutical applications. Powders. 2023;2(2):464-83. doi: 10.3390/powders2020028.
27. Stachurski ZH. On structure and properties of amorphous materials. Materials (Basel). 2011;4(9):1564-98. doi: 10.3390/ma4091564, PMID 28824158.
28. Khajapeer KV, Baskaran KPP R. GC MS and elemental analysis of *Cinnamomumtamala*. Int J Pharm Pharm Sci. 2015;8(8):398-402.
29. Gallington LC, Ghadar Y, Skinner LB, Weber JK, Ushakov SV, Navrotsky A. The structure of liquid and amorphous hafnia. Materials (Basel). 2017;10(11):1290. doi: 10.3390/ma10111290, PMID 29125579.
30. Wu G, Zheng X, Cui P, Jiang H, Wang X, Qu Y. A general synthesis approach for amorphous noble metal nanosheets. Nat Commun. 2019;10(1):4855. doi: 10.1038/s41467-019-12859-2, PMID 31649272.
31. Priemel PA, Grohganz H, Rades T. Unintended and in situ amorphisation of pharmaceuticals. Adv Drug Deliv Rev. 2016;100(1):126-32. doi: 10.1016/j.addr.2015.12.014, PMID 26724250.
32. Jud K, Kausch HH, Williams JG. Fracture mechanics studies of crack healing and welding of polymers. J Mater Sci. 1981;16(1):204-10. doi: 10.1007/BF00552073.
33. Mayerhofer TG, Popp J. Quantitative evaluation of infrared absorbance spectra lorentz profile versus lorentz oscillator. ChemPhysChem. 2019;20(1):31-6. doi: 10.1002/cphc.201800961, PMID 30480862.
34. Butyagin PY. Kinetics and nature of mechanochemical reactions. Russ Chem Rev. 1971;40(11):901-15. doi: 10.1070/RC1971v040n11ABEH001982.
35. Chang JH, Chou CH, Wu JC, Liao KM, Luo WJ, Hsu WL. LCRMP-1 is required for spermatogenesis and stabilises spermatid f-actin organization via the pi3k-akt pathway. Commun Biol. 2023;6(1):389. doi: 10.1038/s42003-023-04778-2, PMID 37037996.
36. Lees G, Stohr T, Errington AC. Stereoselective effects of the novel anticonvulsant lacosamide against 4-AP induced epileptiform activity in rat visual cortex *in vitro*. Neuropharmacology. 2006;50(1):98-110. doi: 10.1016/j.neuropharm.2005.08.016, PMID 16225894.